WWW.IJRPR.COM

International Journal of Research Publication and Reviews

Journal homepage: www.ijrpr.com ISSN 2582-7421

Comparison of Analytical Model for Fiber Impairment Analysis in Optical OFDM

Bekawade Nirbhay Naresh Namrata[a*], Manoj Singh Tomar[b]

[a]*M.Tech Scholar,Department of Electronics and Communication Engineering,School of Research and Technology, People's University, Bhopal, Madhya Prades,462037, India*

[,b]*Associate Professor,Department of Electronics and Communication Engineering, School of Research and Technology, People's University, Bhopal, Madhya Prades,462037, India*

A B S T R A C T

The accuracy of a comprehensive analytical model for analysing the impairments in OFDM-based fibre networks is proven using OptiSystem simulations in this paper. The analytical expression is constructed for expressing the OFDM signal before and after the fibre link. Furthermore, the ASE interactions with fibre nonlinearities are taken into account in the backbone model. The suggested model's performance analysis is presented and contrasted for Dispersion Uncompensated (DUC) and Dispersion Compensated (DC) backbone/backhaul links.

Keywords: OOFDM, CON, AFIM

1. Introduction

A Cognitive Optical Network (CON) is a ground-breaking paradigm that handles the expanding complexity of optical networks while also providing an efficient, user-controlled network. The fundamental idea is to make the network smarter so that it can dynamically adapt to changing network conditions and make decisions based on previous learning. Based on network data and the users' desired Quality of Service, the cognitive optical network planned and makes choices. OFDM stands for Orthogonal Frequency Division Multiplexing and is a type of Multicarrier (MC) modulation used in wireless and cable-based data transport. OFDM has been widely studied in the Radio Frequency (RF) domain, and a recent research called Optical OFDM focuses on using OFDM technology in optical fibre communications (OOFDM). OFDM is well suited to the development of energy-efficient optical BackBone (BB) and Back Haul (BH) systems [12].It's also thought to be a long-term option for allowing flexible resource allocation in Cognitive Optical Networks. Linear and nonlinear errors cascade as the OFDM signal is delivered via optical fibre networks, generating distortion and BER deterioration. As a result, using OFDM in CONs needs precise fibre damage evaluation and irdaptive correction.

2. Literature Review

Baxley, JR, and Zhou, TG, presented two existing distortion-free peak-to-average power ratio (PAR) reduction techniques for orthogonal frequency division multiplexing: selective mapping (SLM) and partial transmit sequence (PTS) [4]. Chung, HS, Chang, SH, and Kim, K shows how to minimize fibre nonlinearity in coherent optical OFDM transmissions using the-law companding transform. A high peak-to-average power ratio (PAPR) in optical fibre intensifies nonlinear effects induced by the Kerr phenomenon [5].

The peak-to-average power ratio (PAPR) of high-order orthogonal frequency-division modulation was studied by Dinur and Wulich. Using studies on level crossing of random processes, an upper bound on the possibility that the PAPR of an OFDM signal would exceed a given value is determined. According to numerical research [6] this bound is tight for low-pass OFDM systems.

Essiambre, RJ, et al. presented a method for determining the capacity limit of fiber-optic communication networks based on information theory (or fibre channels). This paper is divided into two parts. Part 1 delves into the fundamentals of digital communications and information theory. We begin with digitization and modulation, then go on to information theory for both memory-based and non-memory-based channels. [7].

Nag, A., and Wang, T. study the design of an optical network based on orthogonal frequency division multiplexing (OFDM) with the objective of lowering overall network power consumption and making the network green. Mixed-line-rate (MLR) networks, which employ single carrier wavelengths with discontinuous capacity of 10/40/100 Gbps, are another paradigm for tackling traffic heterogeneity and enormous bandwidth needs. In this study, we compare the energy efficiency of an OFDM-based network to an MLR network. [8].

* *Corresponding author.* Tel.: +91-8668291166.
E-mail address: nirbhayb7@gmail.com

Nazarathy, M, investigation of fibre channel Kerr-effect-induced nonlinearities and synthesis of mitigation techniques for these nonlinear (NL) impairments in the context of multicarrier coherent optical Orthogonal Frequency-Division Multiplexing (OFDM) transmission [9].

Ochiai, H investigated the peak-to-average power ratio (PAPR) distribution in severely band-limited orthogonal frequency-division multiplexing (OFDM) transmissions. Assuming that the base-band OFDM signal is a band-limited complicated Gaussian process, we first try to calculate the exact distribution of the PAPR in the band-limited OFDM signals [10].

Pan and colleagues show that by combining the modified Gram-Schmidt method with reorthogonalization techniques, the number of kernels in a Volterra model-based equalizer may be greatly reduced. The resulting "sparse" Volterra model-based electrical equalizer and "complete" Volterra model-based electrical equalizer exhibit comparable performance and can compensate for intra-channel nonlinearity in a 16-QAM 100 Gbit/s CO-OFDM system [11].

Pechenkin, V., and Fair, I.J. proposed optical phase conjugation (OPC) as a method for suppressing such well-matched FWM processes. An analytical formula is developed and described that reliably predicts the degree of suppression. It is demonstrated that, when combined with previously published solutions in the literature, the use of OPC can significantly lower the overall FWM power accumulated within the connection for a wide range of critical design parameters [12].

Peng and colleagues investigate the impact of laser phase noise (PN) in direct-detection optical OFDM (DDO-OFDM) and discover its numerous distinctions from those in coherent optical OFDM (CO-OFDM). Analytical models for various PN effects, such as power degradation, phase rotation term (PRT), and inter-carrier interference (ICI), are provided in terms of important system parameters with and without the tiny PN assumption. [13].

Pham, DT et al. present a numerical and experimental demonstration of the effects of laser phase noise in a direct-detection based optical orthogonal frequency division multiplexing system for access-network transmission, as well as an analysis of system performance in the presence of laser phase noise for different orthogonal frequency division multiplexing symbol durations [14].

Qi, G, and An, VT offer a novel technique for reducing Rayleigh backscattering (RB) and compensating for chromatic dispersion (CD) in a wavelength-division-multiplexed passive optical network (WDM-PON). The suggested correlative level (CL) coding reduces interference generated by RB and CD in the uplink based on reflecting electro-absorption modulator (REAM) [16].

Sina to alleviate nonlinear impairments in fiber-optic systems, Naderi Shahi developed a multi-fiber architecture paired with optical/electrical equalizers. When compared to a single-fiber system, the transmission reach with a BER of 2.1×10-3 is quadrupled in an 8-fiber arrangement [17]. Optical orthogonal frequency division multiplexing (OFDM) signals suffer from the nonlinear effects of an electric-to-optical modulator and fibre due to high peak to average power ratio (PAPR) characteristics, as detailed by Sungyong Kang et al. To lower the PAPR of OFDM, they suggest a power-concentrated subcarrier approach for use in OFDM systems [18].

Wei Wei et al. investigate the efficient delivery of packet and circuit services concurrently in future optical networks, where the software will play an increasing role not only in the control and administration planes but also in the transport plane [19].

Zhu and X investigated an analysis formula for estimating the variance of nonlinear phase noise caused by the interaction of amplified spontaneous emission (ASE) noise with fiber nonlinearity such as self-phase modulation (SPM), cross-phase modulation (XPM), and four-wave mixing (FWM) in coherent orthogonal frequency division multiplexing (OFDM) systems [20].

3. System Model for Fiber Links in Backbone and Backhaul Network

An analytical model is proposed that takes into account various fibre impairments that affect the performance of OFDM transmission over a Back Bone (BB) and Back Haul (BH) network. Figures 1.(a) and 1.(b) exhibit the channel model representations for the BB and BH systems, respectively.

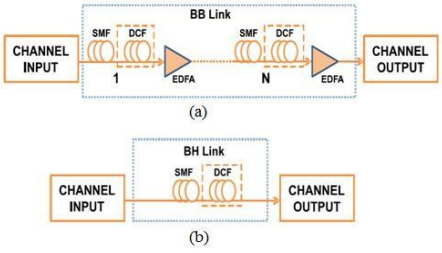

Fig. 1 Channel Model: (a) BB system (b) BH system

The signal from the OFDM transmitter, following RF and optical upconversion, is supplied into the SMF link as the channel input. Because BB networks have fiber lengths in the thousands of kilometres, the optical signal must be boosted and dispersion adjusted on a regular basis. ASE noise generated by the amplifier interacts with fibre nonlinearities during amplification and must be taken into account. The fiber length in BH systems is less than 100 kilometres, and amplifiers are often not required. As a result, in the BH model, the influence of ASE and its related sounds can be ignored. The detailed analytical model for an OFDM-based BB link is described, and the BH model may be deduced by deleting the ASE-related entities.

3.1. Dispersion Uncompensated (DUC) Link

In dispersion uncompensated links, due to improper phase match conditions the effect of FWM is assumed to be negligible. Therefore, in the DUC links it is sufficient to consider fiber dispersion, SPM, XPM and ASE effects. The linearly mapped DD-OFDM signal $s_1(t)$ before propagating into the fiber can be represented as [23];

$$s_1(t) = e^{j2\pi f_0 1} + ae^{j2\pi(f_0+\Delta f)t} . s_B(t) \quad \text{Eqn. 1}$$

where f_0 is the main optical carrier frequency, $\Delta f$is guard band between the main optical carrier and the OFDM band, $\alpha$is the scaling coefficient and $s_B(t)$ is the baseband OFDM signal which can be expanded as;

$$s_B(t) = \sum_{l=-N/2}^{N/2-1} u_l e^{i\omega_l'} \quad \text{Eqn. 2}$$

where u_l is l^{th} information symbol and $\omega_l = 2\pi f_l$ is the angular frequency of l^{th} subcarrier.
For CO-OFDM systems, the transmitted signal $s_2(t)$ can be represented as;

$$S_2(t) = e^{(j2\pi f_{L1} t+\phi_{L1}} . S_B(t) \quad \text{Eqn. 3}$$

where f_{L1} and φ_{L1} are the frequency and phase of the transmitter laser and $s_B(t)$ is the baseband OFDM signal as given in Equation (2).
By considering the effects of dispersion, SPM, XPM and ASE, the received DD-OFDM signal $r_1(t)$ can be derived as;

$$r_1(t) = \{e^{j(2\pi f_0 t+\emptyset(t))} + ae^{j(2\pi(f_0+\Delta f)t+\emptyset(t))} \sum_{I=-\frac{N}{2}}^{N/2-1} \tilde{U}_l(N_a L_a) e^{j2\pi f_l t})\} * \delta(t+T_l) \quad \text{Eqn. 4}$$

where φ(t) represents the phase fluctuation of the laser, Na represents the number of amplifiers, La is the amplifier spacing and the product of Na .La~ gives the total propagation distance, Ul (Na La) represents the complex field of the l th subcarrier at Z = Na La = Ltot and δ(t +Tl) represents the impulse response of fiber dispersion with SPM and XPM. Similarly, the received CO-OFDM signal $r_2(t)$ can be represented as;

$$r_2(t) = \{e^{(j2\pi\Delta F t+\Delta\emptyset)} \sum_{l=-\frac{N}{2}}^{N/2-1} \tilde{u}_l(N_a L_a) e^{j2\pi_l t})\} * \delta(t+T_l) \quad \text{Eqn. 5}$$

where $\Delta F = f_{L1} - f_{L2}$ and $\Delta\varphi = \varphi_{L1} - \varphi_{L2}$ are the frequency and phase difference between the transmit and receive laser. It can be observed from Equations (4) and (5), that the impact of fiber channel impairments is similar for DD-OFDM and CO-OFDM systems. However, a significant spectral efficiency improvement is possible in CO-OFDM by proper choice of modulation, at a cost of increased receiver complexity. In this work, simulations are performed using DD-OFDM to avoid the receiver complexity. The complex field $\tilde{U}_l(N_a L_a)$ in Equation (4) and Equation (5) can be elaborated as;

$$\tilde{U}_I(N_a L_a) = [u_1 + n_I'] \exp\{i\emptyset_{DSX,I} + i\delta\emptyset_{SX,I}\} \quad \text{Eqn. 6}$$

The linear ASE noise n_l is engrafted in the term $\acute{n}_l$ which can be expanded as;

$$n_I' = n_1 \, exp\{-i\emptyset_{DSX,I}\} \quad \text{Eqn. 7}$$

where $\varphi_{DSX,I}$ is the deterministic phase shift due to dispersion, SPM and XPM for the l^{th} subcarrier which has no impact on the nonlinear phase noise and it can be written as;

$$\emptyset_{DSX,I} = -D\pi c N_a L_a \frac{f_l^2}{f_0^2} + \gamma N_a L_{eff} \, (|u_l|^2 + 2\sum_{k\neq 2} |u_k|^2) \quad \text{Eqn. 8}$$

The first term in Eqution (8) represents the phase shift due to dispersion and the second term represents the combined effect of phase shift due to SPM and XPM. Here γ is the nonlinear coefficient, L_{eff} is the effective fiber length and D is the chromatic dispersion with the unit of ps/nm.km.
The second term in the exponent of Equation (6) is the nonlinear phase noise of the l^{th} subcarrier due to SPM and XPM interaction with ASE of N_a amplifiers in the fiber link and is given as;

$$\delta\emptyset_{SX,l} = \gamma L_{eff}[(u_l n_l^* + u_l^* n_l^*) + 2\sum_{k\neq l}(u_k \, n_k^* + u^*{}_k n_k')] \sum_{m=1}^{N_a-1}(N_a - m) \quad \text{Eqn. 9}$$

At the receiver, the photodiode can be modeled as a square law detector and the resultant photocurrent $I_p(t)$ can expressed as;

$$I_p(t) \propto |r_l(t)|^2 = r_1(t) \times r_1(t) \quad \text{Eqn. 10}$$

$$= 1 + 2aRe\{e^{j2r\Delta ft} \sum_{1=-\frac{N}{2}}^{\frac{N}{2}-1} [u_I + n_I'] e^{j\left(2\pi f_1 t+\emptyset_{DSXJ}+\delta\emptyset_{SXJ}+P_I(t)\right)}\}$$

$$+ |a|^2 \sum_{I_1=-\frac{N}{2l_2}}^{\frac{N}{2}-1} \sum_{=-\frac{N}{2}}^{\frac{N}{2}-1} \{[u_{l1} + n_{l1}'][u_{l2}^*$$

$$+ n_{l2}^*] \, e^{j(2\pi(f_{l1}-f_{l\,2})t+\emptyset_{DSXJ\ 1}-\emptyset_{DSX,l2}+\delta\emptyset_{SX,J1}-\delta\emptyset_{SXJ\ 2}+\emptyset(t+T_{l2})-\emptyset(t+T_{I2}))}\}$$

where $\rho_l(t) = \varphi(t + T_l) - \varphi(t)$ is the converted phase fluctuation of the l^{th} subcarrier and $T_l = |\phi_{DSX,l}/2\pi f_l|$ represents the relative time delay between the l^{th} subcarrier and the optical carrier.

In Equation (10), the first term is the direct current that can be easily filtered out. The second term is the fundamental signal consisting of linear OFDM subcarriers which can be sampled and demodulated with Fast Fourier Transform (FFT). The received OFDM symbol is affected by phase noise. The third term is the second-order nonlinearity which can be removed by using RF low pass filtering.

The expression for the output current including photodiode noises can be written as;

$$I(t) = I_p(t) + n_p(t) \quad \text{Eqn. 11}$$
$$where\ n_p(t) = I_d + N_{sh}(t) + N_{th}$$

The expression for the dark current I_d is given as;

$$I_d = I_{sat}\{e^{\frac{q}{K_B T}V_d} - 1\} \quad \text{Eqn. 12}$$

where I_{sat} is the temperature dependent reverse saturation current of photodiode, K_B is the Boltzmann's constant, q is the electronic charge, T is the absolute temperature and V_d is the voltage at the photodiode. The typical value of dark current I_d in the photodiode is 1nA.

The expression for shot noise $N_{sh}(t)$ and thermal noise N_{th} are given as;

$$N_{sh}(t) = \sqrt{2q(I_d + I_p(t))\Delta_f} \quad \text{Eqn. 13}$$

$$N_{th} = \sqrt{\frac{4K_B T\Delta_f}{R_L}} \quad \text{Eqn. 14}$$

where Δ_f is thebandwidth and R_L is the load resistor. The shot noise being signal dependent has a significant impact on the output SNR/EVM and hence affects system throughput [8].

3.2. Dispersion Compensated (DC) Link

In DC links, the dispersion effects are compensated ($D \approx 0$), resulting in phase matched conditions which enhance FWM effects. After considering the effects of SPM, XPM, FWM and ASE, the received signal $r_1(t)$ and $r_2(t)$ can be represented like Equation (15) and Equation (16) ~except for the modified complex field $U_l(N_a L_a)$.

The complex field for DC link is given as;

$$\tilde{u}_l(N_a L_a) = [u_l + n_l']exp[i\emptyset_{SXF,I} + i\delta\emptyset_{F,l} + \xi_{F,l} \quad \text{Eqn. 15}$$

The linear ASE noise is implanted in the term n_l' which can be expanded as;

$$n_l' = n_l exp\{-i\gamma N_a L_{eff}(|u_l|^2 + 2\sum_{k\neq I}|u_k|^2)\} \quad \text{Eqn. 16}$$

where $\emptyset_{SXF,I}$ is the deterministic phase shift due to SPM, XPM and FWM for the l^{th} subcarrier. The modified phase shift equation for DC link ($D \approx 0$) becomes;

$$\emptyset_{SXF,I} = \gamma N_a L_{eff}(|u_l|^2 + 2\sum_{k\neq l}'|u_k|^2) \quad \text{Eqn. 17}$$

The second term in the exponent of Equation (15) is the nonlinear phase noise of the l^{th} subcarrier due to SPM and XPM interaction with ASE represented as in Equation (7).

In Equation (15), $\delta\emptyset_{F,l}$ is the nonlinear phase noise due to ASEFWM interaction and $\xi_{F,l}$ is the deterministic distortion caused by FWM [11].

For DC links, the dispersion factor and the phase mismatch factor will be ideally zero (i.e. fully phase matched). Therefore, the effect of FWM induced distortion and phase noise will tend to a maximum. The modified $\delta\emptyset_{F,l}$ for DC link can be represented as;

$$\delta\emptyset_{F,l} = i\sum_{j=-N2}^{N/2-1}(n_j A_{j,l} + n_j^* B_{j,l} \quad \text{Eqn. 18}$$

where

$$A_{j,l} = \gamma L_{eff}\sum_{i=-N/2}^{N/2-1} u_{j+l-i}u_i^*\sum_{m=1}^{N_a-1}(N_a - m), i \neq j, l \neq +l - j \quad \text{Eqn. 19}$$

$$B_{j,l} = \gamma L_{eff} \sum_{i=-N/2}^{N/2-1} u_{j+l-i} u_i^* \sum_{m=1}^{N_a-1} (N_a - m), i \neq j, l \neq +l - j \quad \text{Eqn. 20}$$

The FWM induced deterministic distortions $\xi_{F,l}$can be modified for DC link as;

$$\xi_{F,l} = \gamma N \ {}_a L_{eff} \sum_{i+J-k=l}^{i\neq l, j\neq k} u_i \, u_j \, u_i^* \quad \text{Eqn. 21}$$

The received OFDM symbol is affected by the additional FWM induced noise compared to the uncompensated link.

4. BER ESTIMATION

The phase noise effects on the received symbol can be mainly categorized as a Power Degradation (PD), Phase Rotation Term (PRT) and Inter Carrier Interference (ICI) mathematically written as;

$$R_l = H_l \, X_l \, \Gamma_l + H_l \ X_l \, \Psi_l \, (0) + H_m \, \mathrm{X}_m \, \Psi_m \, (l - m) \quad \text{Eqn. 22}$$

where X_l and H_l are the transmitted data and channel response respectively. The term Γ_l denotes the PD factor and it can be expressed as;

$$\Gamma_l = l - \eta_l \quad \text{Eqn. 23}$$

where Γ_l is the PN power of the l^{th} subcarrier.
For DUC links, the PN power $\Gamma_l$can be expressed as;

$$\eta_l = 2\pi k T_l + \langle \delta \emptyset_{lin} \rangle^2 + \langle \delta \emptyset_{SX,l} \rangle^2 \quad \text{Eqn. 24}$$

In Equation (24), k indicates the laser linewidth, T_l indicates the relative time delay due to dispersion, SPM and XPM, $\langle \delta \emptyset_{lin} \rangle^2$ is the variance of the linear phase noise due to ASE and $\langle \delta \emptyset_{SX,l} \rangle^2$ is the variance of the nonlinear PN due to SPM and XPM interaction with ASE. The linear and nonlinear PN variances are represented as;

$$\langle \delta \emptyset_{lin} \rangle^2 = \frac{\rho_{ASE} N_a}{2 \, P_{sc} T_{blk}} \quad \text{Eqn. 25}$$

$$\langle \delta \emptyset_{lin} \rangle^2 = \frac{\rho_{ASE} N_a (N_a - 1)(2N_a - 1)\gamma^2 L_{eff}^2 (2N_e - 1) P_{sc}}{3 T_{blk}} \quad \text{Eqn. 26}$$

Whereρ_{ASE} is the ASE power spectral density, N_e is the number of data carrying subcarriers, P_{sc} is the power per subcarrier and T_{blk} is the OFDM symbol duration.
The PN power for DC links is obtained by modifying Equation (24) as;

$$\eta_l = 2\pi \kappa T_l + \langle \delta \emptyset_{lin} \rangle^2 + \langle \delta \emptyset_{SX,l} \rangle^2 + \langle \delta \emptyset_{F,l} \rangle^2 \quad \text{Eqn. 27}$$

where $T_l$indicates the relative time delay due to SPM, XPM and FWM and $\langle \delta \emptyset_{F,l} \rangle^2$ is the variance of PN due to FWM interaction with ASE which can be represented as;

$$\langle \delta \emptyset_{lin} \rangle^2 = \frac{\rho_{ASE} N_a (N_a - 1)(2N_a - 1)\gamma^2 L_{eff}^2 P_{sc}}{12 T_{blk}} \sum_{j=-\frac{N}{2}}^{\frac{N}{2}-1} |2C_{j,l}^* + D_{j,l}|^2 \ + \frac{\rho_{ASE}}{P_{sc} P_{blk}} \, im|B_{l,l}| \quad \text{Eqn. 28}$$

Here;

$$C_{j,l}^* = \sum_{j=-N/2}^{N/2-1} u_{i+l-j}^* u_i, i \neq j, l \neq i + l - j \quad \text{Eqn. 29}$$

$$D_{j,l} = \sum_{j=-N/2}^{N/2-1} u_{j+l-i} \, u_i^*, i \neq j, l \neq i + l - j \quad \text{Eqn. 30}$$

$$B_{l,l} = \frac{\gamma N_a (N_a - 1) L_{eff}}{2} \sum_{j=-N/2}^{N/2-1} u_{2l-i} u_i^*, i \neq l \quad \text{Eqn. 31}$$

From Equation (23), it can be observed that $\Gamma_l + \eta_{l \approx 1}$ which indicates the amount of power loss on the l^{th}subcarrier and is equal to the total PN power. The second term in Equation (22), $\varphi_l(0)$ denotes the PRT on the l^{th} subcarrier. The power of PRT is represented as;

$$\sigma^2_{PRT_l} = \eta_l(\frac{T_1}{T_s N}) \quad \text{Eqn. 32}$$

where T_S is the sampling period and N is number of OFDM subcarriers.
Equation (32) is valid only when the relative time delay is small ($T_l = NT_s$). If the relative time delay is large ($T_l > NT_s$), the PRT power becomes [26];

$$\sigma^2_{PRT_l} = \eta_l - \frac{2\pi\kappa NT_s}{3} \quad \text{Eqn. 33}$$

In addition to power degradation and PRT, the third term in Equation (22), ICI expressed as;

$$\sigma^2_{ICI_l} \leq 1 - (\Gamma_1 + \sigma^2_{PRT_l}) = 1 - (1 - \eta_l + \sigma^2_{PRT_l}) = \eta_l - \sigma^2_{PRT_l} \quad \text{Eqn. 34}$$

Equation (34) holds good only when the relative time delay is small$S_l = N$. If the relative time delay is large (S_l = N -1), the normalized ICI power becomes;

$$\sigma^2_{ICIT_l} = \eta_l - \sigma^2_{PRT_l} = \frac{2\pi\kappa NT_s}{3} \quad \text{Eqn. 35}$$

From the above analysis, the PN power of the l^{th} subcarrier can be approximated as;

$$\eta_l \approx \sigma^2_{PRT_l} + \sigma^2_{ICI_l} \quad \text{Eqn. 36}$$

The ESNR of the l^{th} subcarrier for DUC link can be calculated as;

$$ESNR_l = \frac{\Gamma_1}{\sigma^2_{ICI_l} + |n_p(t)|^2} \quad \text{Eqn. 37}$$

For DC links, the effects of FWM induced deterministic distortions is also included to calculate ESNR. Hence, the ESNR in Equation (37) is modified as;

$$ESNR_l = \frac{\Gamma_l}{\sigma^2_{ICI_l} + \langle\xi_{f,l}\rangle^2 + |n_p(t)|^2} \quad \text{Eqn. 38}$$

where $\langle\xi_{f,l}\rangle^2$ is the variance of FWM induced deterministic distortions and $|n_p(t)|^2$ is the photodiode noise power.
The ensemble ESNR can be obtained by taking the average ESNR over all subcarriers represented as;

$$ESNR = \frac{1}{N}\sum_{l=-N/2}^{N/2-1} ESNR_l \quad \text{Eqn. 39}$$

The BER is estimated from the EVM (Mahmoud et al. 2009) related to the ESNR as;

$$EVM \approx \sqrt{\frac{1}{ESNR}} \quad \text{Eqn. 40}$$

The relationship between the BER and EVM (Shafik et al. 2006) can be represented as;

$$BER_{4Q} = \frac{1}{2} erfc(\sqrt{\frac{1}{2.EVM^2}}) \quad \text{Eqn. 41}$$

where the subscript of BER_{4Q} stands for 4-QAM format and *erfc* represents the complementary error function. As highlighted earlier, the ESNR of the DUC-BB link includes dispersion, SPM, XPM and ASE effects. FWM and its associated interactions is additionally included in the DC-BB link ESNR calculations.
The DUC and DC-BH link ESNRs are derived from the DUC and DC-BB expression by removing the ASE related components. The PN power of the l^{th} subcarrier for DUC and DC-BH links can be represented as;

$$\eta_l = 2\pi\kappa T_l \quad \text{Eqn. 42}$$

Tl varies depending on the deterministic phase shift factor for DC and DUC lines. Because of the balance between linear and nonlinear effects, the quantity of PN power for DUC links is less than for DC lines. Because optical amplifiers are not present in DUC and DC links, the linear and nonlinear PN variances are not considered in total PN power calculations. The remaining steps for determining the output BER are the same as for the BB system. Because of the absence of ASE and its associated interactions, the BER performance of BH networks is projected to be superior than that of BB networks.

5. RESULTS AND DISCUSSION

Numerical estimations of the different impairment parameters derived are carried out to analyse the range of performances of the proposed system model. The results obtained from the proposed model are also compared with an "existing model" which considers only dispersion effects. The various simulation parameters used in the system model are given in Table.1.

Table 1 Simulation parameters

Symbol	Parameter	Value
BR	Bit rate	10 Gb/s
Bps	Bits per symbol (4-QAM)	2
N	Number of OFDM subcarriers	64
f_o	Optical carrier frequency	193.1 THz
f_c	RF carrier frequency	7.5 GHz
f_{ref}	Reference frequency	193.1 THz+7.5 GHz
κ	Laser line width	5 MHz
D	Dispersion	16 ps/nm.km
A_{eff}	Effective fiber cross section	$80\mu m^2$
n_2	Nonlinear index co-efficient	$2.6 \times 10^{-20} m^2/W$
c	Velocity of light in free space	$3x10^8 m/s$
L_{eff}	Effective fiber length	5 Km
L_a	Amplifier spacing	100 Km
N_a	Number of amplifier	10
$N_a . L_a$	Fiber length (For BB)	1000 Km
L	Fiber length (For BH)	100 Km

1.1.1 Performance Evaluation of Fiber Links in BB and BH Networks

This section presents the results of range of performance analysis carried out for BB and BH fiber links with Dispersion Compensation (D=0 ps/nm.km) and without Dispersion Compensation (D = 16 ps/nm.km). Fig. 2.(a) shows the variance of PRT as a function of fiber length for the proposed DUC & DC BB models and the existing model.

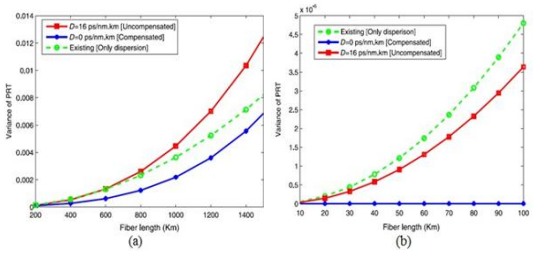

Fig.2 Variance of PRT versus fiber length: (a) BB link (b) BH link

Because of the increased time delay, the PRT power of a DUC link is much higher than the other two scenarios for BB links (Tl). The PRT variance values for the BH scenario are shown in Fig. 2.(b). The results show that the PRT power under dispersion adjustment does not vary because the PN power component is independent of fibre length. Further investigation reveals that, as a result of the suggested comprehensive DUC model's balancing of linear and nonlinear effects, the PRT power is slightly lower than that of the present model. When comparing the BB and BH examples, the results suggest that the quantity of PRT power in the BH system is slightly smaller than in the BB system.

Figures 3.(a) and 3.(b) illustrate the normalised ICI power versus fibre length for the BB and BH links, respectively. The ICI power and total PN power are directly proportional according to Equation (34). In DC-BB lines, the PN power is proportional to the fibre length, whereas it is independent in DC-BH links. Because of the presence of FWM driven interactions and an increase in the linear and nonlinear PN powers in DC links, the overall PN power is larger. As a result, the ICI power of DC-BB linkages is observed to be greater. The normalised ICI power grows significantly with fibre length in uncompensated BH links, although it is smaller than in the existing dispersion only link due to balancing caused by nonlinear generated phase shifts.

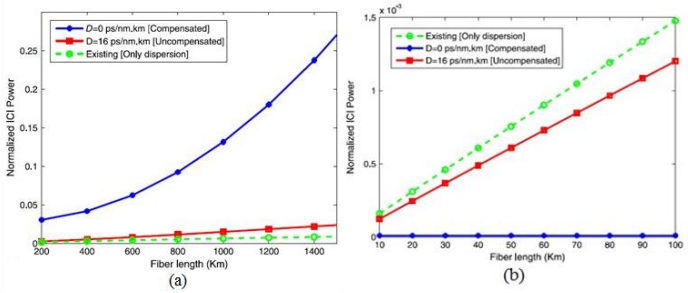

Fig. 3 Normalized ICI power versus fiber length: (a) BB link (b) BH link

For a fixed dispersion of D=16 ps/nm.km, the variation of PRT, ICI and total PN power (constituting the ICI and PRT power), as a function of fiber length is shown for BB and BH links in Fig. 4.(a) and Fig.4.(b) respectively.

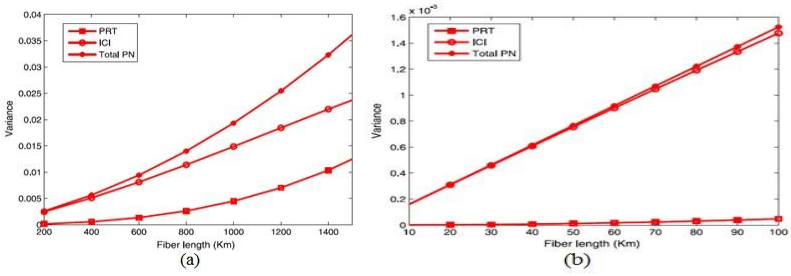

Fig. 4 Normalized ICI power versus fiber length: (a) BB link (b) BH link

With increasing transmission distance, the variance of all parameters studied rises. In BB links, the total PN power is primarily attributable to ICI power at shorter distances, while PRT power begins to increase at longer distances, contributing significantly to the overall PN power. However, in the case of BH linkages, the total PN power is almost entirely attributable to ICI power, with PRT power having a much smaller effect.

6. COMPARISON OF PROPOSED ANALYTICAL LINK MODELS

Table.2 summarises a comparison of the analytical model characteristics produced for backbone and backhaul lines with and without dispersion compensation.

Table 2 Comparison between BB and BH link analytical models

Parameter	BB network			BH network		
	DUC link	DC link	Existing model	DUC link	DC link	Existing model
Dispersion	YES	NO	YES	YES	NO	YES
effects		YES			YES	
SPM	YES	YES	NO	YES	YES	NO
effects			YES			YES
XPM	YES	YES	NO	YES	YES	NO
effects			included			YES
FWM	NO	YES	NO	NO	YES	NO
effects	YES		YES	YES		YES
ASE noise	YES	YES	NO	NO	NO	NO
Dependency on fiber length	Yes	Yes	Yes	Yes	NO	Yes
Dependency on linewidth	Yes	NO	Yes	Yes	Yes	Yes
Dependency on S.C index	Yes	Yes	Yes	Yes	Yes	Yes
Dependency on S.C power	Yes	Yes	NO	NO	NO	NO
PRT power	High	Low	Moderate	Moderate	Low	High
ICI power	Moderate	High	Low	Moderate	Low	High
PN due to time delay	Moderate	Low	High	Moderate	Low	High
PN due to ASE interaction	Low	High	Nil	Nil	Nil	Nil
Total PN power	Moderate	High	Low	Moderate	Low	High
Photodiode noises	YES	YES	YES	YES	YES	YES
Spectral efficiency (b/s/Hz)	0.9812	0.6766	1.0633	1.1809	1.1265	1.1627
BER performance with OFDM	Moderate	Poor	Good	Good	Poor	Moderate
BER performance w/o OFDM	Moderate	Good	Poor	Good	Poor	Moderate

The suggested full-fledged model is also compared to the existing dispersion-only model. The current model implies that system impairments are understated, resulting in good performance for OFDM systems. The comparative study highlights the influence of various fibre impairments on OFDM-based BB and BH network links. Furthermore, the impact of various system factors on different types of linkages is detailed. The spectral efficiency for various links is determined in order to reach the DD-OFDM system's target BER of 10-9. The BER performance of fibre links used in BB and BH networks in the absence of OFDM is also computed and compared. It should be noted that the BER performances in the BH example are the same with or without OFDM.However, in the BB case, particularly in the dispersion adjusted scenario, OFDM-based systems experience significant BER degradation as compared to non-OFDM-based systems. As a result, the suggested model provides useful insight into realistic impairment evaluation in OFDM-based systems.

7. Future Work

This model can be used in the design of Cognitive Optical Networks to accurately identify fiber-related defects.

REFERENCES

[1] Agarwal, GP, "Nonlinear Fiber Optics," 3rd Ed., Academic Press, New York, 2001.
[2] Agarwal, GP, "Fiber Optic communication Systems," Third Edition, John Wiley and Sons, Inc., New York,2002.
[3] Agrawal, GP, "Application of Nonlinear Fiber Optics," Second Edition, Academic Press, USA, 2001.
[4] Baxley, JR & Zhou, TG, "Comparing selected mapping and partial transmit sequence for PAR reduction," IEEE Trans. Broadcasting, vol. 53, no. 4, pp. 797-803, 2008.
[5] Chung, HS, Chang, SH & Kim, K, "Companding transform based SPM compensation in coherent optical OFDM transmission," Opt. Express, vol. 19, no. 26, pp. 702-709, 2011.
[6] Dinur, N & Wulich, D, "Peak-to average power ratio in highorder OFDM," IEEE Trans. Communications, vol. 49, no. 2, pp. 1063-1072, 2001.
[7] Essiambre, RJ, Kramer, G, Winzer, PJ, Foschini, GJ & Goebel, B, "Capacity limits of optical fiber networks," J. Lightwave Technol., vol. 28, no. 4, pp. 662-701, 2010.
[8] Nag, A, Wang T & Mukherjee, B, "Robust design of spectrum efficient green optical backbone networks," J. Lightwave Technol., vol. 31, no. 7, pp. 1138-1144, 2013.
[9] Nazarathy, M & Weidenfeld, R, "Nonlinear impairments in coherent optical OFDM systems and their mitigation," Optical Fiber Communication Reports, vol. 7, pp. 87-175, 2011.
[10] Ochiai, H & Imai, H, "On the distribution of the peak-to-average power ratio in OFDM signals," IEEE Transactionson Communications, vol.49, no.2, pp. 282-289, 2011.
[11] Pan, J & Cheng, CH, "Nonlinear electrical compensation for the coherent optical OFDM system," J. Lightwave Technol., vol. 29, no. 25, pp. 215-221, 2011.
[12] Pechenkin, V & Fair, IJ, "Analysis of four-wave mixing suppression in fiber-optic OFDM transmission systems with an optical phase conjugation module," Journal of Opt. Commun. Netw., vol. 2, no. 9, pp.701-710, 2010.
[13] Peng, WR, "Analysis of laser phase noise effect in direct-detection optical OFDM transmission," J. Lightwave Technol., vol. 28, no. 17, pp. 2526–2536, 2010.
[14] Pham, DT et al., "Laser phase noise and OFDM symbol duration effects on the performance of direct-detection based optical OFDM access network," Opt. Fiber Technol., vol.17, no.3, pp.252–257, 2011.
[15] Proakis, JG, "Digital Communications," Third edition, McGrawHill, New York, 1995.
[16] Qi, G & An, VT, "Mitigation of Rayleigh noise and dispersion in REAM-based WDM-PON using spectrum shaping codes," Opt.Express, vol. 20, no. 26, pp. 452-461,2012.
[17] Sina Naderi Shahi & Shiva Kumar, "Reduction of nonlinear impairments in fiber transmission system using fiber and/or transmitter diversity," Optics communications, vol. 285, pp. 3553-3558, 2012.
[18] Sungyong Kang, Jaehoon Lee & Jichai Jeong, "PAPR reduction technique by inserting a power concentrated subcarrier for COOFDM," Opt. Commun., vol. 35, pp. 119-123, 2015.
[19] Wei Wei, Chonggang Wang & Jianjun Yu, "Cognitive Optical Networks: Key Drivers, Enabling Techniques and Adaptive Bandwidth Services," IEEE Communications Magazine, vol. 50, no. 1, pp. 106-113, 2012.
[20] Zhu, X & Shiva Kumar, "Nonlinear phase noise in coherent optical OFDM transmission systems," Opt. Express, vol. 18, no. 7, pp.7347-7360, 2010.